

C3A Cells-Inoculated Affinity Membrane for Bilirubin Removal

Yuqing Shen ^{1,†} , Huijuan Liu ^{2,†}, Huiling Luo ², Xinxin Liu ², Yanan Sun ², Dongtao Ge ^{2,*} and Wei Shi ^{2,*}

¹ Department of Transfusion, Woman and Children's Hospital, School of Medicine, Xiamen University, Xiamen 361003, China

² The Higher Educational Key Laboratory for Biomedical Engineering of Fujian Province/Research Center of Biomedical Engineering of Xiamen, Department of Biomaterials, College of Materials, Xiamen University, Xiamen 361005, China

* Correspondence: gedt@xmu.edu.cn (D.G.); shiwei@xmu.edu.cn (W.S.)

† These authors contributed equally to this work.

Abstract: Affinity membranes have the potential to enhance the specific adsorption of toxins, however, they suffer from insufficient hemocompatibility and low therapeutic efficiency during blood detoxification therapy. Herein, we combine an affinity membrane with a bioreactor to develop a blood purification membrane with affinity adsorption detoxification and cell detoxification functions. To fabricate the membrane, a polyethersulfone (iPES) membrane with a macroporous support layer was prepared by a phase inversion technique and modified with polydopamine (PDA). The iPES/PDA composite membrane exhibited excellent biocompatibility and blood compatibility, as well as controllable permeability. Lysine (Lys) and hepatocytes (C3A cells), which were selected as the affinity ligand for bilirubin adsorption and detoxification cells, respectively, were immobilized on the iPES/PDA composite membrane via the active group and adhesiveness of PDA coating on the membrane. The fabricated C3A cells-inoculated iPES/PDA/Lys membrane not only achieved high cell activity and function of the inoculated cells but also significantly improved the toxin clearance efficiency.

Keywords: polydopamine; affinity membrane; polyethersulfone; adsorption



Citation: Shen, Y.; Liu, H.; Luo, H.; Liu, X.; Sun, Y.; Ge, D.; Shi, W. C3A Cells-Inoculated Affinity Membrane for Bilirubin Removal. *Coatings* **2023**, *13*, 50. <https://doi.org/10.3390/coatings13010050>

Academic Editor: Anton Ficai

Received: 19 November 2022

Revised: 22 December 2022

Accepted: 22 December 2022

Published: 27 December 2022



Copyright: © 2022 by the authors. Licensee MDPI, Basel, Switzerland. This article is an open access article distributed under the terms and conditions of the Creative Commons Attribution (CC BY) license (<https://creativecommons.org/licenses/by/4.0/>).

1. Introduction

Affinity membranes are an ideal separation technology for the purification and recovery of biomolecules since they integrate the dual advantages of separation by microfiltration and affinity adsorption [1]. Since affinity adsorption often happens in mild conditions such as the environment in the human body, it is expected to be fit for the selective removal of toxins in patients with autoimmune diseases. In addition to excellent specific adsorption, the advantages that affinity membranes offer compared to conventional hemoperfusion are the short diffusion paths and low-pressure drops [2]. For these reasons, affinity membranes should potentially improve therapeutic efficiency and reliability in blood detoxification [2–4]. However, the binding rate of toxin and the hemocompatibility of the affinity membrane are insufficient for blood detoxification therapy.

Biological artificial liver (BAL) is a system wherein liver cells are cultivated in an in vitro bioreactor. When the patient's blood flows through the reactor, it exchanges substances with the liver cells in the reactor, which perform detoxification, synthesis, and biotransformation [5–7]. Compared with traditional nonbiological artificial livers, BALs not only have a liver-specific detoxification function, but can also participate in the metabolism of three substances (sugar, protein, and fat) and secrete substances that promote the growth of liver cells, which can effectively replace the detoxification function and synthesis function of the liver. Although the existing bioartificial liver reactor system to some extent realizes the detoxification and biosynthesis functions of the liver, it is difficult to detoxify a large number of metabolites and toxic substances accumulated in the body of patients with liver failure by cultured liver cells, which may also have adverse effects on the survival and

biological functions of the cells [8–12]. Therefore, the development of an efficient bioreactor that can effectively detoxify and maintain cell activity would significantly improve the efficiency of blood detoxification.

In this paper, we combined an affinity membrane and a bioreactor, and fabricated a blood purification membrane with affinity adsorption detoxification and cell detoxification functions, for the first time. To facilitate the immobilization of affinity ligands and the inoculation of hepatocytes, we prepared polyethersulfone (iPES) asymmetric membranes with macroporous support layers and modified them with polydopamine (PDA). PDA can be formed by self-polymerization of dopamine aqueous solution under alkaline conditions (Figure 1a) [13]. PDA has a good adhesion property and can adhere to the surfaces of many inorganic and organic materials to form an extremely thin film. It has shown a good application prospect in the fields of biomaterial coating [14–16], drug release [17–20], and biosensors [21–23]. Existing studies have confirmed that a matrix modified with PDA can adhere to cells well and maintain cell activity and function [13–15]. In addition, PDA also contains a large number of active groups, which can react with biological molecules through a Michael addition reaction or Schiff base reaction (Figure 1b) [13–16]. This is conducive to the immobilization of affinity ligands. Herein, bilirubin was chosen as a representative of protein-bound toxins. A hepatocytes-inoculated affinity membrane was fabricated by immobilizing lysine (Lys) and inoculating C3A cells on the PDA-coated iPES membrane via the active groups and adhesiveness of PDA, where Lys was the affinity ligand for bilirubin and C3A cells were the detoxification cells. The hemocompatibility of the membranes and the adsorption capacity of bilirubin were investigated. It is found that the C3A cell-inoculated affinity membranes excellently retained cell activity, successfully achieved functionalization of the inoculated cells, and significantly improved toxin clearance efficiency. Our results not only reveal C3A cells-inoculated affinity membranes as a promising candidate for bilirubin removal but also provide a potential mode for blood purification.

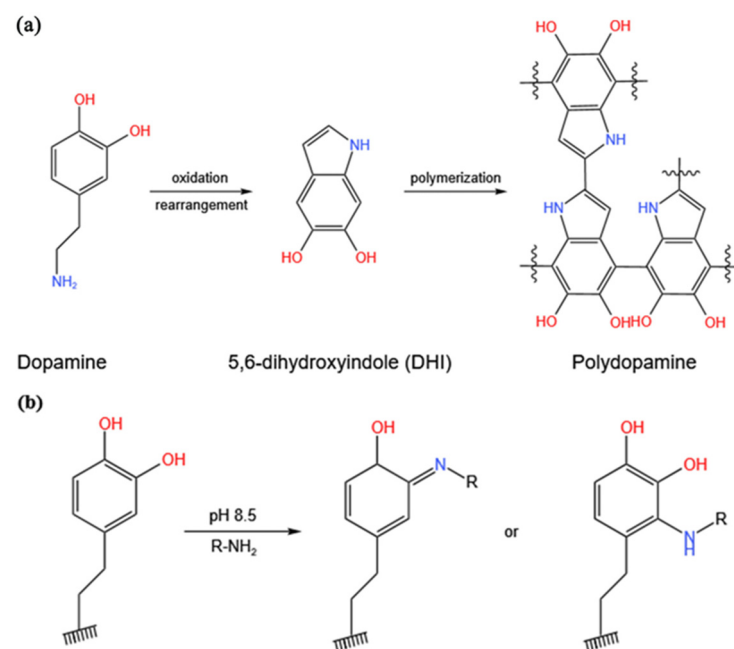


Figure 1. (a) Polymerization of dopamine; (b) Chemical modification of polydopamine via a Schiff base reaction or Michael addition reaction.

2. Materials and Methods

2.1. Materials

Polyethersulfone (iPES, Ultrason E6020P, BASF) and lysine (Lys) were obtained from Sinopharm Chemical Reagent Co., Ltd. (Shanghai, China). Dopamine hydrochloride (DA·HCl)

was purchased from Yuancheng Technology Development Co., Ltd. (Wuhan, China). Polyvinyl pyrrolidone (PVP-K30) and polyethylene glycol (PEG-1000) were acquired from Xiamen Green Glass Instrument Co., Ltd. (Xiamen, China). N-N dimethylacetamide was purchased from J&K Scientific Ltd. (Beijing, China). Tris(hydroxymethyl)aminomethane, bovine serum albumin (BSA, fraction V, 95%), and 3-(4,5-Dimethylthiazol-2-yl)-2,5-diphenyl tetrazolium bromide (MTT) were acquired from Sigma-Aldrich Chemical Co., Ltd. (St. Louis, MO, USA). Partial thromboplastin reagent and Test-Thromborel reagent were purchased from Shanghai Sun Biotechnical Limited Company (Shanghai, China). All the aqueous solutions were prepared with deionized water (DI water).

2.2. Membrane Preparation and Modification

The iPES ultrafiltration membranes applied in this study were prepared by a phase inversion technique according to our earlier method [24]. Briefly, 2.7 g iPES, 0.15 g PEG-1000, and 1.65 g PVP were dissolved in 11 mL N, N-dimethylacetamide. The polymer solution was stirred at 60 °C for 24 h, followed by stewing for 24 h to remove air bubbles. Then, the solution was cast onto a clean glass plate with 100 µm thickness using a casting knife [25]. Afterward, the glass plate was immediately immersed in a coagulation bath (deionized water) at 20 °C, where an exchange of solvent and non-solvent occurred, and left for 1 day. Finally, the membranes (iPES) were extensively washed with deionized water and dried in a vacuum.

Before modifying, the iPES membranes were cut into squares with a side length of 2.5 cm. Then, the membranes were immersed in the solution of 2 mg/mL DA·HCl at pH 8.5 (Tris buffer). The solution was shaken vigorously and conducted at 25 °C. After 24 h of polymerization, the polydopamine (PDA) functionalized iPES membrane (iPES/PDA) was washed with 0.5 M NaCl solution and double-distilled water.

The further modification was based on the catechin group of PDA. The iPES/PDA membranes were taken into the potassium carbonate and sodium bicarbonate buffer solution containing 9 mg/mL Lys at 40 °C for 5 h by shaking vigorously. After the reaction, the Lys-immobilized membranes (iPES/PDA/Lys) were washed in 0.5 M NaCl and water extensively. The amount of the Lys coupled onto the iPES/PDA/Lys membrane was determined by detecting the absorbance of the Lys solution before and after the reaction at 268 nm using a UV-VIS spectrophotometer (UV1750).

2.3. Characterization of Membranes

The surface morphologies of the uncoated and coated iPES membranes were observed by a Field-emission scanning electron microscope (FE-SEM) (Field Emission, SU70, Hitachi, Tokyo, Japan). The chemical bonds or functional groups of iPES, PDA, Lys, iPES/PDA, and the iPES/PDA/Lys membranes were analyzed by ATR-FTIR (Nicolet IN10, Thermo Fisher Scientific, Waltham, MA, USA). The static contact angle between the membrane surfaces and water or whole blood was measured by a contact-angle goniometer (DSA100, Dataphysics Instruments GmbH, Filderstadt, Germany). Briefly, 3 µL of ultrapure water or whole blood was dropped on the surface of the membranes at room temperature, and the contact angle was measured after 5 s.

2.4. Permeability of Membranes

The flux of pure water was measured by a dead-end ultrafiltration cell. Before testing, the membrane with an effective diameter of 25 mm was pre-compacted at 0.1 MPa for 1 h, and the flux of pure water was measured at room temperature and pressure (0.1 MPa). The flux (J) was calculated by the following equation:

$$J(\text{mL}/\text{cm}^2\text{h}) = \frac{V}{St} \quad (1)$$

where V is the volume of water through the membrane in a given time t and S is the effective membrane area.

A 1 mg/mL BSA solution was pumped into the dead-end ultrafiltration cell containing a pre-compacted membrane by a peristaltic pump at room temperature and pressure (0.1 MPa). The BSA rejection ratio (R) was calculated by Equation (2):

$$R = \left(1 - \frac{C_p}{C_f}\right) \times 100\% \quad (2)$$

where C_f and C_p are the concentrations of the feed and permeate solution of BSA, respectively. The concentration of BSA was measured by a UV-VIS spectrophotometer at 280 nm.

2.5. Blood Coagulation Time Tests

To evaluate the antithrombogenicity of the membranes, the activated partial thromboplastin time (APTT) and the thrombin time (TT) were measured using a coagulation analyzer (GF-2000, Shandong Gaomi Caihong Analytical Instrument Co., Ltd., Weifang, China). Human whole blood gathered from a healthy person was attenuated with 3.8% sodium citrate solution (9:1 dilution). The platelet-poor plasma (PPP) was obtained by centrifuging at 4000 rpm for 15 min at 4 °C. The membranes ($1 \times 1 \text{ cm}^2$ each) were incubated in 500 μL PBS at 37 °C for 1 h, then the PBS was taken away and 500 μL PPP was added. After incubating at 37 °C for 1 h, 100 μL PPP was added into the test cup, then mixed with 100 μL APTT agent (incubated at 37 °C before use) and put into a rolling ball mill. After incubating at 37 °C for 5 min, 100 μL of 0.025 M CaCl_2 solution was added, followed by measuring the APTT with a coagulation analyzer. The test method of TT was similar to that of APTT [26].

2.6. Hemolysis

The membranes were previously incubated in 5 mL of normal saline at 37 °C for 30 min. A 100 μL sample of the anticoagulant whole blood was added, then mixed gently and incubated for 60 min. Similarly, 100 μL of anticoagulant whole blood was incubated in 5 mL of 0.1% Na_2CO_3 for 1 h at 37 °C, and the solutions were set as positive and negative controls, respectively. After centrifuging for 5 min at 3000 rpm, the absorbance (A) of the supernatant of all the samples was measured at 540 nm. The percent hemolysis was calculated as follows [27]:

$$\text{Percent hemolysis} = \frac{A_{\text{test}} - A_{\text{negative control}}}{A_{\text{positive control}} - A_{\text{negative control}}} \times 100 \quad (3)$$

2.7. Cell Viability

2.7.1. MTT

C3A human immortalized liver cells (ATCC, Manassas, VA, USA) were cultured in RPM1640 medium replenished with 10% fetal bovine serum (FBS, Gibco, Waltham, MA, USA) at 37 ± 1 °C in 5% CO_2 . The culture medium was replaced every day.

The membranes were pre-wetted by immersion in 48-well plates with the culture medium for 3 h in a 37 °C incubator and irradiated in an ultraclean workbench for 12 h. The toxicity of the membranes to C3A cells was determined by MTT assay. A cell suspension was made at a density of 2.0×10^4 cells/mL. A 1 mL sample of this cell suspension was added to each culture and cultured in DMEM supplemented with 10% FBS and 1% penicillin-streptomycin at 37 °C in 5% CO_2 . Cells cultured without membranes served as controls. After culturing for 24 or 48 h, the supernatant of each unit was removed and the cells were rinsed three times with PBS. A 100 μL sample of MTT solution (5 mg/mL in PBS) and 500 μL fresh DMEM/FBS were then added and incubated for 4 h. The formed precipitates were dissolved in 100 μL dimethyl sulfoxide. After 30 min, the absorbance intensity was then read at 570 nm using a microplate reader Pro-200 (Tecan, Männedorf, Switzerland). The relative cell viability (mean% \pm SD, $n = 3$) was expressed as $\text{Abs}_{\text{sample}} / \text{Abs}_{\text{control}} \times 100\%$.

2.7.2. C3A Cells Inoculation

The membranes were incubated in a 1 mL cell suspension of C3A cells (2.0×10^4 cells/mL) at 37 °C for 48 h. After rinsing the membrane with PBS to remove non-adherent cells, the membranes were immersed in 2.5% glutaraldehyde solution in PBS for 30 min, dehydrated with a series of ethanol/water (wt%) mixtures (50%, 60%, 70%, 80%, 90%, and 100%) and dried at room temperature. C3A cells inoculated on the membranes were observed by SEM.

2.8. Bilirubin Adsorption Experiments

The Lys-attached affinity membranes (iPES/PDA/Lys) were tested for the adsorption of bilirubin in bilirubin–BSA solution, which was used to simulate a patient's plasma of hyperbilirubinemia. Since the bilirubin is easily oxidized by exposure to direct sunlight or any other source of ultraviolet light, including fluorescent lighting, the adsorption experiments were executed in a dark room. The amounts of bilirubin adsorbed were determined as follows:

$$Eq = \frac{(C_i - C_t)V}{S} \quad (4)$$

where Eq is the amount of bilirubin adsorbed onto a unit area of the membrane (mg/cm^2); C_i is the initial concentration of the bilirubin (mg/mL); C_t is the concentration of the bilirubin after adsorption (mg/mL); V is the volume of the bilirubin solution (mL); and S is the area of the membrane (cm^2). The membranes (15 cm^2) were immersed in 10 mL bilirubin–BSA solution at 37 °C. At the specified time, the concentration of bilirubin in the solution was measured by spectrophotometry at the wavelength of 460 nm.

2.9. Determination of Albumin and Urea

The secretion of albumin from the C3A cells was tested by an enzyme-linked immunosorbent assay (ELISA, Thermo Fisher Scientific, Waltham, MA, USA). The secretion of urea from the C3A cells was measured by Urea Assay Kit (Abnova, Taipei, Taiwan). Data are expressed as the means \pm SD of four independent measurements.

2.10. Bilirubin Clearance

The two-compartment cell was separated by the C3A cell-inoculated affinity membrane. One compartment facing the permselective layer of the membrane contained the plasma of patients with jaundice, and the other facing the macroporous support layer of the membrane was the culture medium. At the specified time, the concentration of bilirubin in the plasma was measured by a Beckman Coulter Synchron[®] clinical system DXC800 (Beckman-Coulter, Brea, CA, USA). The iPES and iPES/PDA/Lys membranes without inoculation of C3A cells were set as the control group. The clearance rate of bilirubin was calculated as follows:

$$Q = \frac{C_i - C_t}{C_t} \quad (5)$$

where Q is the clearance rate of bilirubin; C_i is the initial concentration of bilirubin; and C_t ($\mu\text{mol}/\text{L}$) is the concentration of bilirubin after adsorption.

3. Results and Discussion

3.1. Characterization

It is well known that iPES ultrafiltration membranes prepared by the phase inversion method have the typical asymmetric structure containing a dense layer and a support layer. The surface morphologies of the PES membranes are shown in Figure 1, revealing the smooth surface of the dense layer (Figure 2a) and exposed large holes ($\sim 20 \mu\text{m}$) of the support layer (Figure 2b). To improve the biocompatibility of the membrane and strengthen the inoculation of cells on the membrane, PDA was used to modify the PES membrane. Dopamine can polymerize to form thin adherent PDA coatings on any surface, including organic and inorganic surfaces [28]. The quinone groups on PDA can react with thiol compounds and nitrogen derivatives [28], which help to immobilize biological

molecules and cells. After 24 h modified by PDA, we can see the lamellar structure of PDA on the dense layer of the iPES membrane, and some particles also appeared in the pores (Figure 2c,d). These results indicate that the PDA was ornamented on the surface as well as on the pore walls, forming a PDA coating on both the dense and support layers of the iPES. This process mainly depended on the adhesion of the PDA. Figure 3 shows the ATR-FTIR spectra of the iPES substrate, PDA, Lys, iPES/PDA, and iPES/PDA/Lys composite membranes. The PDA peak at 1610 cm^{-1} was attributed to the aromatic rings stretching vibrations and N–H bending vibrations, and a broad peak at approximately 3360 cm^{-1} was assigned to the catechol hydroxyl group and N–H groups. Compared with the spectra of PDA, the iPES/PDA membranes showed the same broad peak between 3500 and 3200 cm^{-1} , which was attributed to the stretching vibrations of the N–H/O–H, and the peak at 1610 cm^{-1} which was attributed to the aromatic rings stretching vibrations and N–H bending vibrations [29]. The peaks at 1650 cm^{-1} , $2800\text{--}3000\text{ cm}^{-1}$, and $3100\text{--}3500\text{ cm}^{-1}$ of free Lys, which were attributed to the carboxyl vibration peak, C–H stretching vibration peak, and N–H stretching vibration peak, appeared in the spectrum of the iPES/PDA/Lys, indicating that Lys was loaded on the iPES/PDA membranes successfully. Moreover, the peak of iPES/PDA/Lys at 1520 cm^{-1} , which was attributed to the --C=N-- generated by the Schiff base reaction (Figure 1b) between Lys and PDA, indicated that Lys was covalently immobilized onto the iPES/PDA membranes.

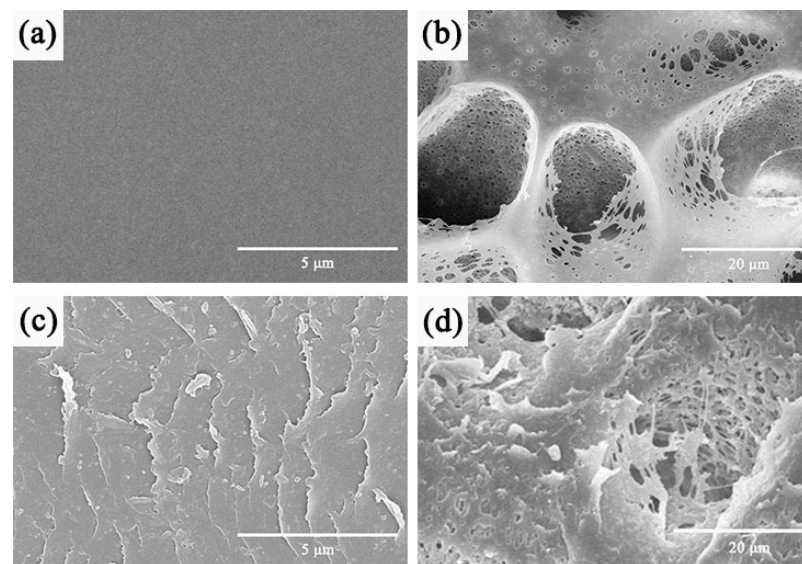


Figure 2. SEM images of the surface of the iPES membrane ((a), Dense layer; (b), Support layer), and iPES/PDA composite membrane ((c), Dense layer; (d), Support layer).

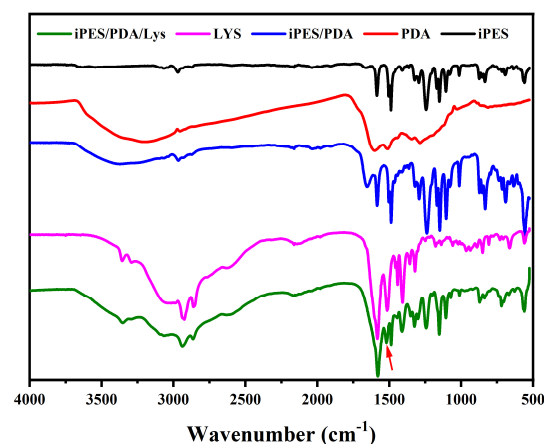


Figure 3. ATR-FTIR spectra of iPES, PDA, Lys, iPES/PDA, and the iPES/PDA/Lys composite membranes.

3.2. Membrane Performance

Coating PDA on the iPES membrane changes the permeability of the membrane. Before measuring the water flux of the membrane, we observed the color change of the composite membrane after the polymerization of polydopamine. With the increase in polymerization time of PDA, the color of the iPES/PDA composite membrane gradually deepened (Figure 4a), indicating that the amount of PDA coated on the iPES membrane increased. Figure 4b shows the effect of the polymerization time of PDA on water flux and protein retention ratio. The flux for the original iPES membrane was about 75.2 mL/(cm²·h). After coating by PDA, the water flux decreased sharply in the first 12 h. When the coating time of PDA is between 12 h to 24 h, the water flux did not greatly change, approaching 3.3 mL/(cm²·h) at 24 h. Figure 4b also shows the time-dependent BSA rejection ratio. The BSA rejection ratio of the original iPES membrane (PDA coating time: 0 h) was about 78%. The rejection ratio increased rapidly with the increase in coating time of PDA in the first 12 h, and gradually plateaued (90%) when the coating time reaches 12 h (Table S1). These can be attributed to the decrease in membrane permeability due to the increase in the thickness of the PDA coating [29]. To assess the hydrophilic–hydrophobic properties of the membrane surfaces, water contact angles were measured at different coating times. Figure 4c shows the water contact angle decreased with the increase in the PDA coating time (from 89.3° to 58.2°), indicating that the polydopamine coating is beneficial to improve the hydrophilicity of the iPES membrane, which is attributed to an increase in the number of catechin hydroxyl groups in PDA. Based on the water flux, protein retention ratio, and hydrophilicity of the membrane, we chose the membrane coated with PDA for 12 h to carry out the subsequent bilirubin clearance and blood compatibility evaluation.

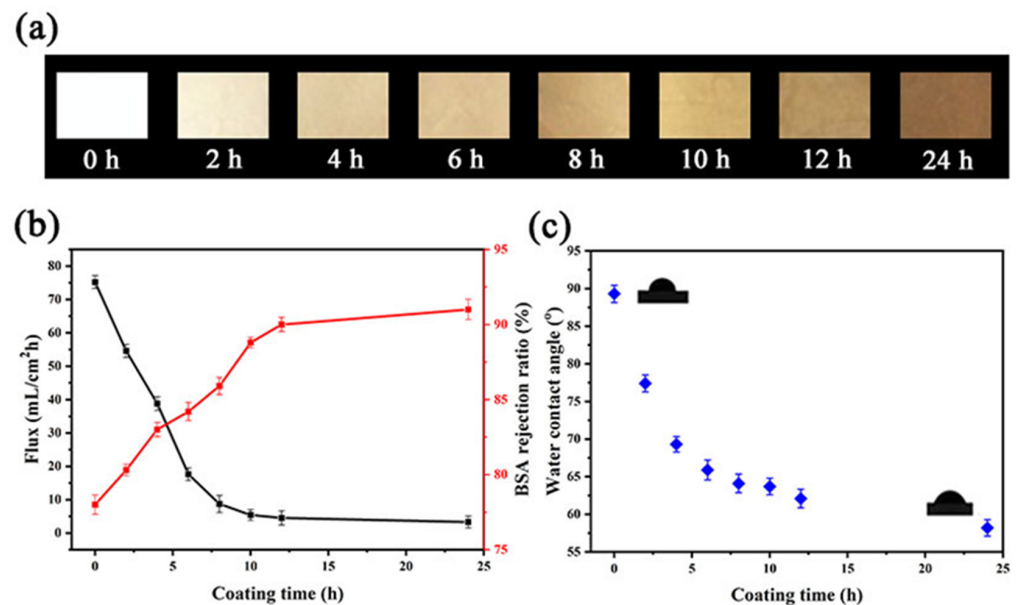


Figure 4. (a) Digital photo of iPES membranes with different coating times of PDA; (b) Effect of PDA coating time on the water flux and BSA rejection ratio of iPES/PDA composite membrane; (c) Effect of PDA coating time on the water contact angle of iPES/PDA composite membrane.

3.3. Hemocompatibility Studies

3.3.1. Blood Contact Angle

Since the BAL system is in direct contact with blood, we first evaluated the blood wettability of the membrane. Table 1 shows that the blood wettability was enhanced after PDA and Lys modification of the iPES membranes, as shown by the decrease in blood contact angle from 89° to 38°, which benefits the reduction of the non-specific adsorption of biomolecules and enhance the hemocompatibility of the membrane.

Table 1. The blood contact angle of the membranes.

Membrane	Contact Angle (°)
iPES	89 ± 7
iPES/PDA	58 ± 3
iPES/PDA/Lys	38 ± 5

3.3.2. Blood Coagulation

The antithrombogenicity of the membranes was evaluated by blood coagulation time tests. The blood coagulation cascade included the intrinsic, extrinsic pathway, and common pathways [30]. The intrinsic and common pathways can be evaluated by APTT. The extrinsic and common pathways can be evaluated by TT. The APTT and TT of the membranes are shown in Figure 5. The result of APTT demonstrated that the iPES membrane has an endogenous anticoagulant effect to some extent. After modification by PDA and Lys, the effect of endogenous anticoagulant was enhanced obviously, especially after grafting of Lys. For the modified membranes (iPES/PDA/Lys), lots of catechol hydroxyl groups on the PDA and the anionic groups -COOH in the Lys, which were abundant on the surface of the membranes, were available for binding coagulation factors, and they could interfere with the blood clotting process. Similar to heparin, the polydispersed anionic might bind and catalyze the interaction of plasma proteins involved in the intrinsic clotting cascade, which helps to prolong clotting time [31]. However, it can be seen from the TT results that the iPES/PDA and iPES/PDA/Lys membranes do not show enhanced exogenous anticoagulation, which indicates that the modified membranes cannot interfere with the exogenous pathway.

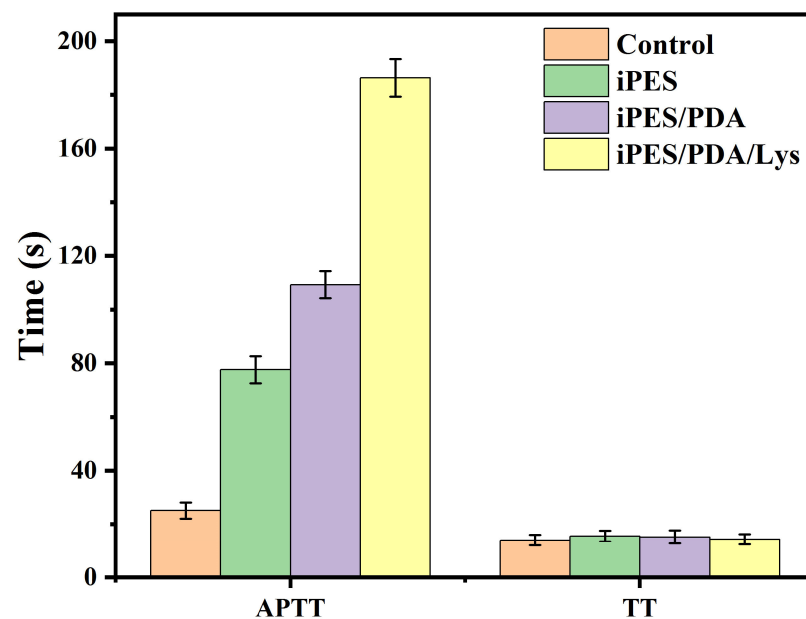


Figure 5. APTT and TT assays for the iPES, iPES/PDA and iPES/PDA/Lys membranes. The results are expressed as means ± SD (n = 3).

3.3.3. Hemolysis

Hemolysis is the breakage of red blood cells with the release of hemoglobin to the surrounding fluid. Table 2 listed the hemolysis ratio of the iPES, iPES/PDA, and iPES/PDA/Lys membranes. It can be seen that the iPES/PDA and iPES/PDA/Lys membranes were more hemocompatible than the iPES membranes, and belong to the categories of highly hemocompatible biomaterials (<5% hemolysis) [27]. This further proves that the iPES/PDA/Lys membranes have excellent blood compatibility.

Table 2. Hemolysis rate of the membranes.

Sample	Optical Density	Hemolysis%
Positive control	0.151	100
Negative control	0.005	0
iPES	0.015	6.9
iPES/PDA	0.011	4.1
iPES/PDA/Lys	0.009	2.8

3.4. Adsorption of Bilirubin

The adsorption rate curves of bilirubin are shown in Figure 6a. The results show that relatively fast adsorption rates were observed at the beginning of the adsorption process, and then the adsorption equilibrium was achieved gradually at the third hour (Table S2). This figure also shows the difference in adsorption capacity between the iPES, iPES/PDA, and iPES/PDA/Lys membranes. The iPES membrane has the lowest non-specific bilirubin adsorption ($4.0 \mu\text{g}/\text{cm}^2$), and this adsorption may be due to the weak hydrophobic interaction between bilirubin and the iPES membrane. After coating PDA on the iPES membrane, the adsorption capacity of the composite membrane increased to $9.8 \mu\text{g}/\text{cm}^2$. This increased adsorption can be attributed to the excellent adhesion performance of PDA. To enhance specific bilirubin adsorption, Lys was chosen as the affinity ligand, and immobilized onto the iPES/PDA membrane. The fabricated iPES/PDA/Lys affinity membrane achieved the highest adsorption capacity of bilirubin ($15.53 \mu\text{g}/\text{cm}^2$). The effect of bilirubin initial concentration on adsorption capacity is shown in Figure 6b and Table S3. The adsorption capacity of the membranes initially increased with the increase in the initial concentration of bilirubin and reached equilibrium when the bilirubin concentration was greater than 200 mg/mL, indicating that the adsorption sites on the membrane have been occupied by bilirubin.

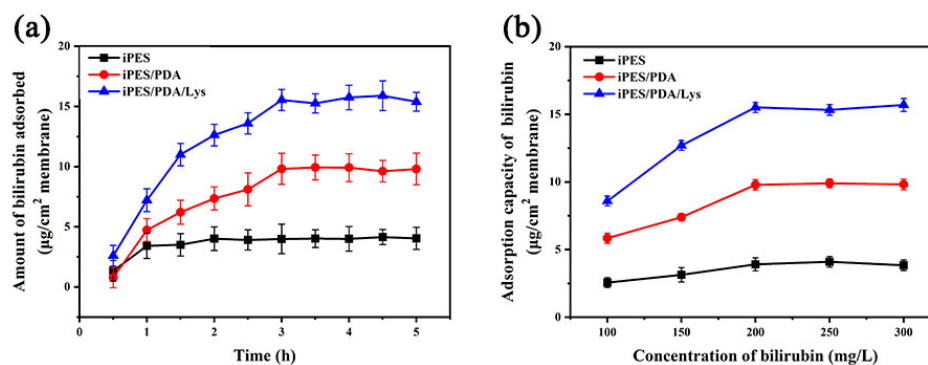


Figure 6. (a) Adsorption rates of bilirubin on the membranes. Initial bilirubin concentration: 200 mg/L. (b) The effect of bilirubin initial concentration on the adsorption capacities. Adsorption time: 3 h. The results are expressed as means \pm SD ($n = 3$).

3.5. In Vitro Cytotoxicity

Before inoculating C3A cells on the membrane, we first investigated the cytotoxicity of the membrane to the cells. As shown in Figure 7, the pristine iPES membrane had a slightly increased toxicity to the cells compared with the control, but the iPES/PDA and iPES/PDA/Lys membranes retained better viability during the whole culture time. They not only have no cytotoxicity but can also promote cell growth, which indicated that modification with PDA and Lys has a positive effect on the cytocompatibility of the membranes [26,32]. Figure 8 shows the growth morphology of C3A cells on the membrane surface. The adhesion and growth state of the C3A cells in the blank group (glass) surface is relatively good. However, due to the hydrophobicity of the iPES membrane surface, the C3A cells on the iPES membrane surface are relatively sparse. Compared with the iPES membrane, the iPES/PDA membrane is more favorable for the adhesion and

growth of C3A cells. It is worth noting that the adhesion and growth state of C3A cells on the iPES/PDA/Lys affinity membrane surface is the best, which is due to the strong adhesion of PDA and the hydrophilic properties of Lys. It is gratifying that C3A cells firmly attached to the membrane pores in the support layer surface, which not only avoids the shedding of cells but also provides a three-dimensional environment for the growth of C3A cells. Therefore, iPES/PDA/Lys membranes inoculated with C3A cells are conducive to maintaining cell activity and their function.

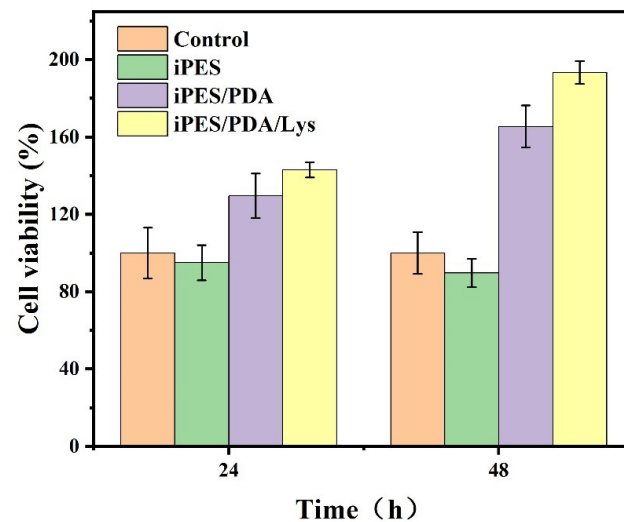


Figure 7. Cell viability of C3A after incubation with the membranes for 24 h and 48 h. Values are expressed as means \pm SD (n = 4).

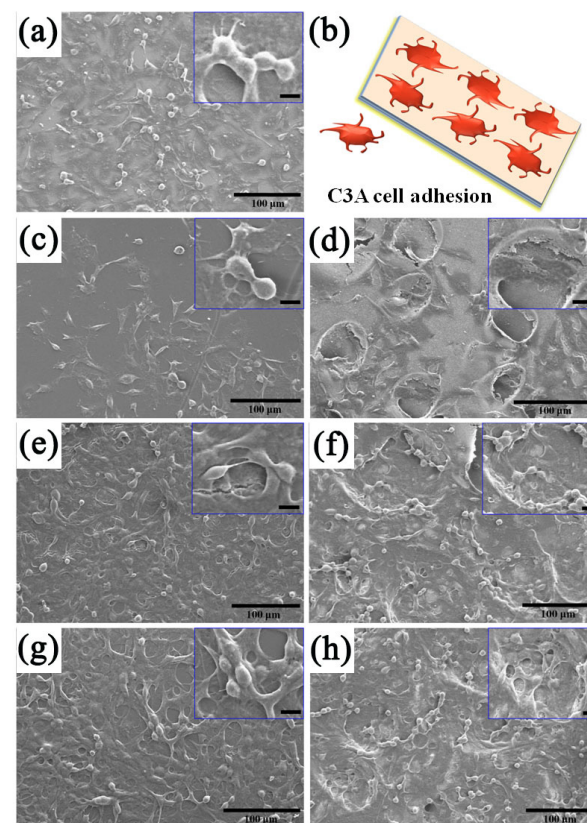


Figure 8. SEM images of C3A cell adhesion on glass (a), iPES ((c), Dense layer; (d), Support layer), iPES/PDA (e), Dense layer; (f), Support layer), and iPES/PDA/Lys ((g), Dense layer; (h), Support layer). (b) Schematic diagram of C3A cells adhesion on the surface of the membrane.

3.6. Cell Functionality and Bilirubin Clearance

Albumin secretion and urea synthesis are liver-specific functions. To evaluate the functional activity of the C3A cells inoculated on the membranes, the concentrations of albumin and urea were measured in the supernatant on the 2nd, 4th, 6th, and 8th days. The content of secreted albumin and synthesized urea in all C3A cell-inoculated membranes increased with incubation time (Figure 9). Significantly more albumin and urea were secreted and synthesized by the C3A cells grown on the iPES/PDA/Lys membranes than those grown on the iPES and iPES/PDA membranes, and the produced albumin and urea of the C3A cell-inoculated iPES/PDA/Lys membranes on the 8th day were 4.2 $\mu\text{g/L}$ and 43 $\mu\text{g/L}$, which were about 3.5- and 2.0-fold of C3A cell-inoculated iPES membranes, respectively.

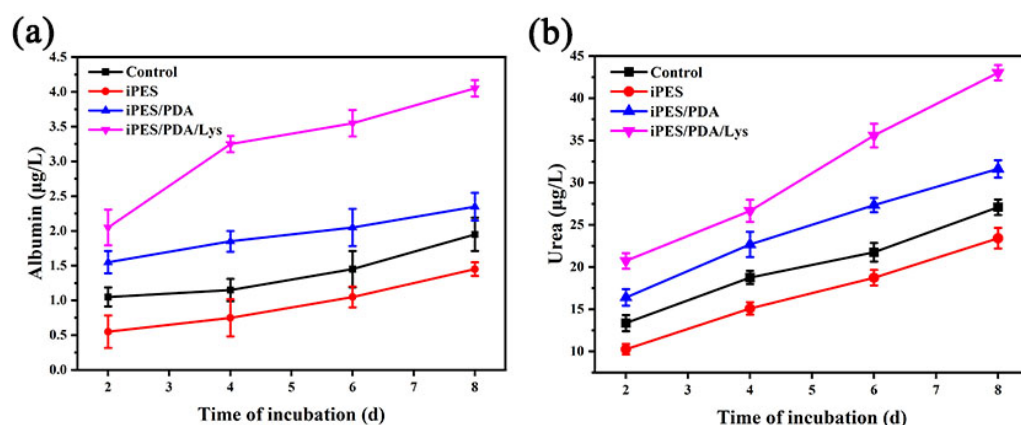


Figure 9. Albumin secretion (a) and urea formation (b) of C3A cells inoculated on the membranes. Control groups were treated without membranes. The values are expressed as means \pm SD ($n = 3$).

To confirm the combined clearance effects of affinity adsorption and cell detoxification, the removal of bilirubin from the plasma of patients with jaundice was performed. The bilirubin clearance rate of the iPES and iPES/PDA/Lys membranes with and without inoculation of C3A cells are listed in Table 3. The iPES/PDA/Lys membrane inoculated with C3A cells exhibited the highest clearance rate of bilirubin (41.7%). This can be attributed to the following two aspects: on the one hand, the iPES/PDA/Lys membrane contains an adhesive coating of PDA and the affinity ligand Lys, which can absorb more bilirubin molecules; and, on the other hand, the iPES/PDA/Lys membrane can be inoculated with more C3A cells, which can absorb more bilirubin and achieve a biological detoxification function.

Table 3. Bilirubin removal rate of the membranes from plasma of patients with jaundice.

Sample	With Inoculation of Cells Removal Rate	Without Inoculation of Cells Removal Rate
iPES	14.2%	6.9%
iPES/PDA/Lys	41.7%	23.4%

4. Conclusions

In summary, the C3A cell-inoculated iPES/PDA/Lys membranes that have the dual functions of affinity adsorption and cell detoxification were fabricated and used for bilirubin removal. The water flux, retention ratio, and hydrophilicity of the iPES/PDA membranes can be regulated by changing the polymerization time of PDA. The iPES/PDA membranes showed good biocompatibility, blood compatibility, and adhesion performance, which were conducive to the immobilization of affinity ligands and cell inoculation. These characteristics ensured the activity and function of the inoculated cells, as well as efficient bilirubin clearance.

Supplementary Materials: The following are available online at <https://www.mdpi.com/article/10.3390/coatings13010050/s1>, Table S1: The effect of PDA coating time on the absorbance of BSA permeate solution; Table S2: Adsorption rates of bilirubin on the membranes; Table S3: The bilirubin concentrations before and after adsorption with membranes.

Author Contributions: Conceptualization, Y.S. (Yuqing Shen), H.L. (Huijuan Liu), D.G. and W.S.; Methodology, Y.S. (Yuqing Shen), H.L. (Huijuan Liu), H.L. (Huiling Luo), W.S., Y.S. (Yanan Sun) and D.G.; Investigation, Y.S. (Yuqing Shen), H.L. (Huijuan Liu), X.L., Y.S. (Yanan Sun) and H.L. (Huiling Luo); Data analysis, X.L. and Y.S. (Yanan Sun); Writing—Original Draft, Y.S. (Yuqing Shen) and H.L. (Huijuan Liu); Writing—Review & Editing, Y.S. (Yuqing Shen), H.L. (Huiling Luo), D.G. and W.S.; Funding Acquisition, W.S., Y.S. (Yanan Sun) and Y.S. (Yuqing Shen); Supervision, W.S. and D.G.; H.L. (Huijuan Liu) and W.S. oversaw all research. All authors have read and agreed to the published version of the manuscript.

Funding: This research was funded by the National Natural Science Foundation of China (22172132, 31870986, 31271009), the Natural Science Foundation of Fujian Province of China (2021J01041, 2020J01036), the Program for New Century Excellent Talents in University, and the Foundation of Xiamen Science and Technology Bureau (3502Z20209206).

Institutional Review Board Statement: The study was conducted in accordance with the Declaration of Helsinki, and approved by the Ethics Council of Human Research in Xiamen Maternal and Child Health Care Hospital (protocol code: KY-2020-111 and date of approval: 8 January 2021).

Informed Consent Statement: Informed consent was obtained from all subjects involved in the study.

Data Availability Statement: Data available on request from the authors.

Conflicts of Interest: The authors declare no conflict of interest.

References

1. Zou, H.; Luo, Q.; Zhou, D. Affinity membrane chromatography for the analysis and purification of proteins. *J. Biochem. Biophys. Methods* **2001**, *49*, 199–240. [[CrossRef](#)]
2. Xue, M.Q.; Ling, Y.S.; Wu, G.S.; Liu, X.; Ge, D.T.; Shi, W. Surface-modified anodic aluminum oxide membrane with hydroxyethyl celluloses as a matrix for bilirubin removal. *J. Chromatogr. B* **2013**, *912*, 1–7. [[CrossRef](#)]
3. Charcosset, C. Membrane Processes in biotechnology: An overview. *Biotechnol. Adv.* **2006**, *24*, 482–492. [[CrossRef](#)]
4. Shi, W.; Cao, H.-H.; Song, C.F.; Jiang, H.R.; Wang, J.; Jiang, S.H.; Tu, J.; Ge, D.T. Poly(pyrrole-3-carboxylic acid)-alumina composite membrane for affinity adsorption of bilirubin. *J. Membr. Sci.* **2010**, *353*, 151–158. [[CrossRef](#)]
5. Anand, A.; Mallick, S.P.; Singh, B.N.; Kumari, S.; Suman, D.K.; Tripathi, S.; Singh, D.; Srivastava, P. A critical aspect of bioreactor designing and its application for the generation of tissue engineered construct: Emphasis on clinical translation of bioreactor. *Biotechnol. Bioprocess Eng.* **2022**, *27*, 494–514. [[CrossRef](#)]
6. Tuerxun, K.; He, J.Y.; Ibrahim, I.; Yusupu, Z.; Yasheng, A.; Xu, Q.L.; Tang, R.H.; Aikebaier, A.; Wu, Y.Q.; Tuerdi, M. Bioartificial livers: A review of their design and manufacture. *Biofabrication* **2022**, *14*, 032003. [[CrossRef](#)]
7. Wang, J.L.; Ren, H.Z.; Liu, Y.X.; Sun, L.Y.; Zhang, Z.H.; Zhao, Y.J.; Shi, X.L. Bioinspired artificial liver system with hiPSC-derived hepatocytes for acute liver failure treatment. *Adv. Healthc. Mater.* **2021**, *10*, 2101580. [[CrossRef](#)]
8. Soto-Gutierrez, A.; Kobayashi, N.; Rivas-Carrillo, J.D.; Navarro-Alvarez, N.; Zhao, D.B.; Okitsu, T.; Noguchi, H.; Basma, H.; Tabata, Y.; Chen, Y.; et al. Reversal of mouse hepatic failure using an implanted liver-assist device containing ES cell-derived hepatocytes. *Nat. Biotechnol.* **2006**, *24*, 1412–1419. [[CrossRef](#)]
9. Kulig, K.M.; Vacanti, J.P. Hepatic tissue engineering. *Transpl. Immunol.* **2004**, *12*, 303–310. [[CrossRef](#)]
10. Maringka, M.; Giri, S.; Bader, A. Preclinical characterization of primary porcine hepatocytes in a clinically relevant flat membrane bioreactor. *Biomaterials* **2010**, *31*, 156–172. [[CrossRef](#)]
11. Kinasiewicz, A.; Smietanka, A.; Dudzinski, K.; Chwojnowski, A.; Gajkowska, B.; Werynski, A. Spongy polyethersulfone membrane for hepatocyte cultivation: Studies on human hepatoma C3A cells. *Artif. Organs* **2008**, *32*, 747–752. [[CrossRef](#)] [[PubMed](#)]
12. Zhang, Y.; Shi, X.L.; Han, B.; Gu, J.Y.; Chu, X.H.; Xiao, J.Q.; Ren, H.Z.; Tan, J.J.; Ding, Y.T. The influence of membrane molecular weight cutoff on a novel bioartificial liver. *Artif. Organs* **2012**, *36*, 86–93. [[CrossRef](#)] [[PubMed](#)]
13. Lee, H.; Dellatore, S.M.; Miller, W.M.; Messersmith, P.B. Mussel-inspired surface chemistry for multifunctional coatings. *Science* **2007**, *318*, 426–430. [[CrossRef](#)] [[PubMed](#)]
14. Lee, Y.B.; Shin, Y.M.; Lee, J.H.; Jun, I.D.; Kang, J.K.; Park, J.C.; Shin, H. Polydopamine-mediated immobilization of multiple bioactive molecules for the development of functional vascular graft materials. *Biomaterials* **2012**, *33*, 8343–8352. [[CrossRef](#)]
15. Yang, K.; Lee, J.S.; Kim, J.; Lee, Y.B.; Shin, H.; Um, S.H.; Kim, J.B.; Park, K.I.; Lee, H.; Cho, S.W. Polydopamine-mediated surface modification of scaffold materials for human neural stem cell engineering. *Biomaterials* **2012**, *33*, 6952–6964. [[CrossRef](#)] [[PubMed](#)]

16. He, Y.; Dai, L.F.; Zhang, X.M.; Sun, Y.N.; Shi, W.; Ge, D.T. The bioactive polypyrrole/polydopamine nanowire coating with enhanced osteogenic differentiation ability with electrical stimulation. *Coatings* **2020**, *10*, 1189. [[CrossRef](#)]
17. Wang, W.; Zheng, J.Y.; Zhou, H.; Liu, Q.; Jia, L.; Zhang, X.M.; Ge, D.T.; Shi, W.; Sun, Y.N. Polydopamine-based nanocomposite as a biomimetic antioxidant with a variety of enzymatic activities for Parkinson's disease. *ACS Appl. Mater. Interfaces* **2022**, *14*, 32901–32913. [[CrossRef](#)]
18. Liu, Y.L.; Ai, K.L.; Liu, J.H.; Deng, M.; He, Y.Y.; Lu, L.H. Dopamine-melanin colloidal nanospheres: An efficient near-infrared photothermal therapeutic agent for in vivo cancer therapy. *Adv. Mater.* **2013**, *25*, 1353–1359. [[CrossRef](#)]
19. Liu, X.; Xie, Z.; Shi, W.; He, Z.; Liu, Y.; Su, H.L.; Sun, Y.N.; Ge, D.T. Polynorepinephrine nanoparticles: A novel photothermal nanoagent for chemo-photothermal cancer therapy. *ACS Appl. Mater. Interfaces* **2019**, *11*, 19763–19773. [[CrossRef](#)]
20. Chen, F.H.; Zhang, X.C.; Wang, Z.N.; Xu, C.S.; Hu, J.Z.; Liu, L.; Zhou, J.C.; Sun, B.W. Dual-responsive and NIR-driven free radical nanoamplifier with glutathione depletion for enhanced tumor-specific photothermal/thermodynamic/chemodynamic synergistic therapy. *Biomater. Sci.* **2022**, *10*, 5912–5924. [[CrossRef](#)]
21. Ruan, C.Q.; Shi, W.; Jiang, H.R.; Sun, Y.N.; Liu, X.; Ge, D.T. One-pot preparation of glucose biosensor based on polydopamine-graphene composite film modified enzyme electrode. *Sens. Actuators B Chem.* **2013**, *177*, 826–832. [[CrossRef](#)]
22. Li, Y.X.; Luo, L.X.; Nie, M.Y.; Davenport, A.; Li, Y.; Li, B.; Choy, K.L. A graphene nanoplatelet-polydopamine molecularly imprinted biosensor for ultratrace creatinine detection. *Biosens. Bioelectron.* **2022**, *216*, 114638. [[CrossRef](#)] [[PubMed](#)]
23. Jaime, J.; Rangel, G.; Munoz-Bonilla, A.; Mayoral, A.; Herrasti, P. Magnetite as a platform material in the detection of glucose, ethanol and cholesterol. *Sens. Actuators B Chem.* **2017**, *238*, 693–701. [[CrossRef](#)]
24. Shi, W.; Zhang, F.B.; Zhang, G.L.; Jiang, L.Q.; Wang, S.L.; Xu, H. Facilitated transport of lipophilic toxins through polysulfone membrane using albumin as a carrier. *Mol. Simulat.* **2004**, *30*, 117–120. [[CrossRef](#)]
25. Zinadini, S.; Zinatizadeh, A.A.; Rahimi, M.; Vatanpour, V.; Zangeneh, H. Preparation of a novel antifouling mixed matrix PES membrane by embedding graphene oxide nanoplates. *J. Membr. Sci.* **2014**, *453*, 292–301. [[CrossRef](#)]
26. Ma, L.; Qin, H.; Cheng, C.; Xia, Y.; He, C.; Nie, C.X.; Wang, L.R.; Zhao, C.S. Mussel-inspired self-coating at macro-interface with improved biocompatibility and bioactivity via dopamine grafted heparin-like polymers and heparin. *J. Mater. Chem. B* **2014**, *2*, 363–375. [[CrossRef](#)]
27. Khan, W.; Kapoor, M.; Kumar, N. Covalent attachment of proteins to functionalized polypyrrole-coated metallic surfaces for improved biocompatibility. *Acta Biomater.* **2007**, *3*, 541–549. [[CrossRef](#)]
28. Lee, H.; Rho, J.; Messersmith, P.B. Facile conjugation of biomolecules onto surfaces via mussel adhesive protein inspired coatings. *Adv. Mater.* **2009**, *21*, 431–434. [[CrossRef](#)]
29. Cheng, C.; Li, S.; Zhao, W.F.; Wei, Q.; Nie, S.Q.; Sun, S.D.; Zhao, C.S. The hydrodynamic permeability and surface property of polyethersulfone ultrafiltration membranes with mussel-inspired polydopamine coatings. *J. Membr. Sci.* **2012**, *417*, 228–236. [[CrossRef](#)]
30. Lin, W.C.; Liu, T.Y.; Yang, M.C. Hemocompatibility of polyacrylonitrile dialysis membrane immobilized with chitosan and heparin conjugate. *Biomaterials* **2004**, *25*, 1947–1957. [[CrossRef](#)]
31. Ran, F.; Nie, S.Q.; Li, J.; Su, B.H.; Sun, S.D.; Zhao, C.S. Heparin-like macromolecules for the modification of anticoagulant biomaterials. *Macromol. Biosci.* **2012**, *12*, 116–125. [[CrossRef](#)] [[PubMed](#)]
32. Nie, S.Q.; Tang, M.; Cheng, C.; Yin, Z.H.; Wang, L.R.; Sun, S.D.; Zhao, C.S. Biologically inspired membrane design with a heparin-like interface: Prolong blood coagulation, inhibited complement activation, and bio-artificial liver related cell proliferation. *Biomater. Sci.* **2014**, *2*, 98–109. [[CrossRef](#)] [[PubMed](#)]

Disclaimer/Publisher's Note: The statements, opinions and data contained in all publications are solely those of the individual author(s) and contributor(s) and not of MDPI and/or the editor(s). MDPI and/or the editor(s) disclaim responsibility for any injury to people or property resulting from any ideas, methods, instructions or products referred to in the content.